

# Picosecond Fluorescence Studies by Intracavity Gain Spectroscopy in a Modelocked Dye Laser<sup>★</sup>

H. Bettermann<sup>★★</sup> and G. Chini

Institut für Physikalische Chemie und Elektrochemie, Heinrich-Heine-Universität Düsseldorf, Geb. 26.43., W-4000 Düsseldorf, Fed. Rep. Germany

Received 7 October 1991/Accepted 12 December 1991

**Abstract.** This article presents measurements which combine modelocking technique with intracavity spectroscopy. To test this approach, a sample ( $10^{-5}$  M ethanolic solution of 1,4-dihydroxyanthraquinone) was inserted in a modelocked Ar<sup>+</sup> ion laser and probed by intracavity pulses of a synchronously pumped dye laser. The probing of the sample results in an amplification of the dye laser output. Maximum output was measured if the pulses of the dye laser temporally overlapped with those of the Ar<sup>+</sup> ion laser inside the sample. Under this condition, the spectral laser intensity was shaped by the spectrum of stimulated fluorescence which originated from a molecular vibronic state populated by pump laser excitation.

**PACS:** 31.50, 32.50, 31.70

The recording of transient species can basically be divided into two experimental configurations: those, in which the detector has proper time resolution for direct measurements of short-time events and those, in which the investigated compound is sampled by studying the alterations of a second pulse (probe pulse) delayed in time from an initiating pulse (pump pulse) as a function of time delay between these considered pulses. In the latter case of pump-probe spectroscopy, no time resolution of the detectors is required. This technique has been extensively used and is well documented in monographs concerning ultrafast spectroscopy [1, 2]. Using highly repetitive, stable laser devices such as modelocked cw dye lasers, the probe-pulse data from numerous events are collected and averaged.

In this article, we present a modified version of this high-repetition-rate pump and probe technique in which the sample being investigated is inserted in the cavity of a modelocked laser.

Measurements of samples placed inside laser cavities have been usually performed in cw dye lasers to determine small sample absorbances [3, 4] or to observe optical gain provided by fluorescence of sample molecules [5]. Intracavity absorption measurements are normally carried out using gaseous samples to activate mode competition processes [6]. Mode competition between absorbing and non-absorbing resonator modes generates large enhancements of absorption sensitivity so that sample concentrations of  $5 \times 10^5$  particles/cm<sup>3</sup> are

detectable [7]. Using special experimental conditions, these large absorption enhancements can also be measured in the case of liquid samples, although the large bandwidths of the absorption bands do not promote competition processes [8]. Nevertheless, in comparison with single path measurements outside laser resonators, liquid samples inserted in laser cavities normally increase the detectability by three orders of magnitude. Placing additional gain media inside a dye laser cavity, optical gains in the range of about  $2 \times 10^{-5}$  are detectable [9]. The recording of these small gains could be achieved by operating near laser threshold.

This article deals with the experimental setup and spectroscopic results of intracavity gain experiments. We investigated amplification properties of ethanolic solutions of quinizarin (1,4-dihydroxyanthraquinone). This compound has been subject of numerous investigations concerning the behaviour of molecular luminescence since quinizarin can be regarded as a parent molecule for a number of compounds exerting biological activity by the formation of intercalation complexes inside the double helix structure of DNA [10].

## 1 Experimental Method

The combination of modelocking technique with intracavity spectroscopy was tested by inserting a sample within a modelocked and cavity dumped dye laser. Intracavity absorptions in a cavity-dumped dye laser whose resonator was prepared for modelocking operations has been carried out previously [11]. In that experiment general conditions of in-

<sup>★</sup> Presented at LASERION '91, June 12–14, 1991, München (Germany)

<sup>★★</sup> Author to whom correspondence should be addressed

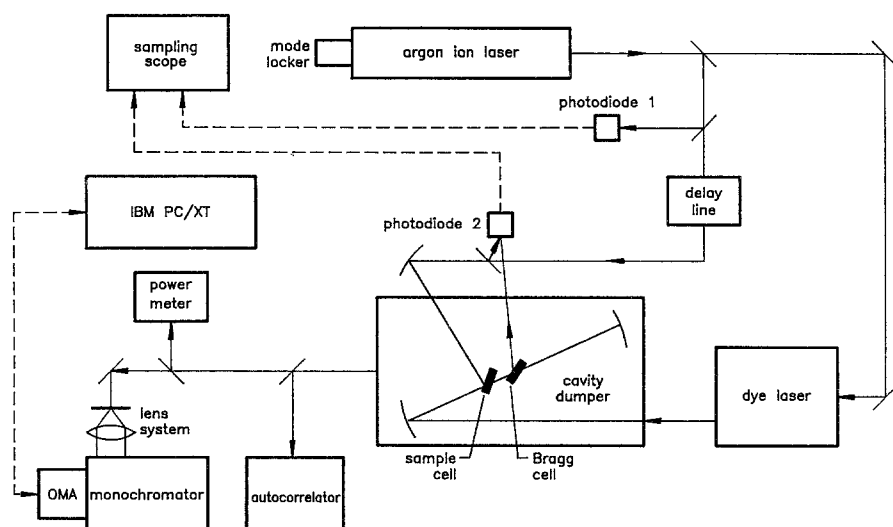


Fig. 1. Experimental setup

tracavity absorption measurements of liquid samples were studied and the spin-forbidden  $S_0-T_1$  transition in pyrene molecules was quantitatively recorded.

In highly repetitive pulse systems (e.g., modelocking lasers with 82 MHz repetition frequency) absorption measurements are hardly successful if the initially occupied molecular singlet states are subject to the investigations because of the continuous population of the longer-living lowest triplet states. For this reason, the investigation of excited singlet states is concentrated on intracavity experiments which utilize stimulated emission of the sample. This approach has been carried out by simultaneous excitation of the sample with pulses of a modelocked laser which synchronously excited the chosen dye laser. Interrogating the sample with intracavity dye laser pulses, the excited sample molecules are radiatively deactivated. This yields an increase of the outcoupled pulse intensity. The wavelength-dependent alterations of this light-amplifying process caused by the fluorescence properties of the inserted sample can then be investigated by varying the frequency of the dye laser. The magnitude of light amplification generated by the fluorescing sample depends sensitively on the alignment of the excitation laser beam within the sam-

ple cell. If the focus of the excitation laser beam does not spatially overlap with the dye laser beam, the intensity of the dye laser beam is only weakened by effects of intracavity absorption.

The experimental setup is schematically shown in Fig. 1. The sample cell was mounted on the Bragg cell housing between the folding mirror of the cavity dumper and the optico-acoustic modulator (Fig. 2). To avoid reflections of the intracavity laser beam which would totally impair mode-locking, the cell was Brewster-angle aligned. In this part of the resonator, the dye laser beam is chamfered by the focusing folding mirror of the cavity-dumper assembly and the generation of induced fluorescence is surely supported by the increased photon density. The insertion of the sample cell slightly modifies the optical path in the dye laser resonator. To match the altered length of the resonator to the repetition frequency of the pump laser pulses, the cavity dumper housing is mounted on a translation stage.

To control the adjustment of the temporal shift between the pump laser pulses and intracavity pulses, parts of both beams are directed to photodiode 2 (Fig. 1) and monitored synchronously. During each round-trip the intracavity dye

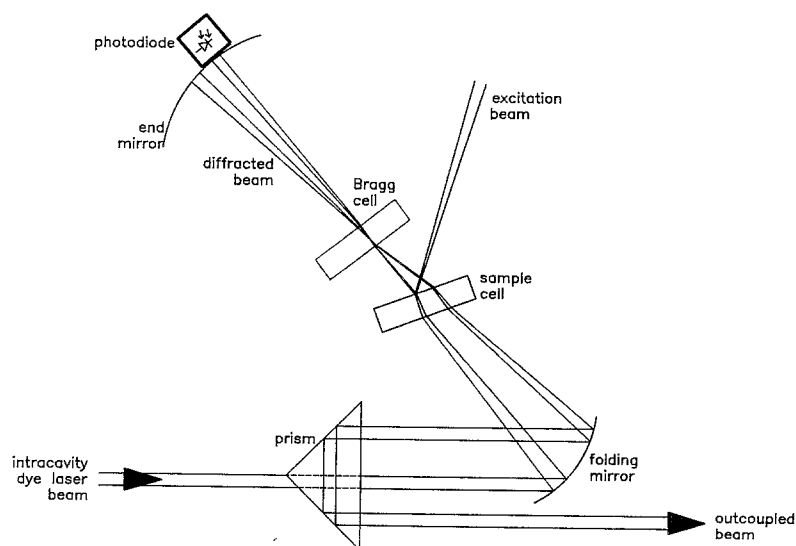


Fig. 2. Assembly of the sample. The optical components (end mirror, folding mirror, Bragg cell, and prism) belong to the cavity dumper. The photodiode behind the end mirror is used to synchronize dye laser pulses with pump laser pulses

laser beam traverses the sample cell two times. According to the distance between sample cell and end mirror of the cavity dumper assembly, the back reflected pulse reaches the cell about 800 ps after its first pass. To avoid two interrogations of the sample molecules by the intracavity beam during one round-trip, the temporal shift between the pulses which excite the sample and those of the dye laser is related to the back-travelling pulses.

## 2 Apparatus and Sample Preparation

The dye laser was pumped by a modelocked argon ion laser (Spectra Physics model 171, 514.5 nm; repetition frequency: 81.847 MHz; FWHM: 250 ps, 900 mW average power). The pulses of the argon ion laser were recorded with a photodiode (UDT Sensors, model HS 008 with self-built circuit) and displayed on a sampling scope (Hewlett Packard model 185B with 187B dual trace plug-in unit). For a pump power of 450 mW, the sample-containing dye laser (threshold: pump power of about 200 mW) generated an output power of 1.5 mW (30 W peak power). The repetition frequency of the outdumped dye laser pulses was chosen to be 4 MHz. The FWHM of the outcoupled dye laser pulses was determined to be 10 ps using a self-built autocorrelator (SHG with angle-tuned KDP; aligned for  $553 \pm 1$  nm; the device was calibrated with glass plates of different thickness). The autocorrelation trace was detected on a real time scope (Tektronix model 5B10N). A small fraction of the outcoupled laser beam was directed to a pyroelectric power meter (Coherent radiation power meter, model 212) to control the average output power of the dye laser.

Single-line operation of the dye laser was achieved by the insertion of three wavelength-selecting elements inside the dye laser resonator: a tuning wedge (free spectral range (FSR): 100 THz at 580 nm), an etalon (FSR: 900 GHz at 580 nm), and an excess etalon (plate for microscopy, thickness 50  $\mu$ m). With absent excess etalon, the dye laser generated up to eleven lines (the number of lines depends on the chosen wavelength) spaced by the free spectral range of the etalon. A combination of monochromator (Jobin Yvon, model THR 1500; polychromator version with absent exit slit) and a non-gated optical multichannel analyser (PAR, model OMA II, vidicon tube; SIT 1254) was used to detect the output power of the dye laser. Data processing and the control of the multichannel analyzer were carried out by a slightly modified IBM/XT which was adapted for rapid data transmission using a self-constructed data-transfer device [12]. The spectra of amplified laser power were measured in steps of 0.67 nm.

To adjust the time delay between excitation pulses and the intracavity pulse train, an optical delay line was placed between argon ion laser and sample cell. The delay line covered a range of about 3 ns. A beamsplitter (50% reflectance) positioned near the output mirror of the argon ion laser directed the outcoupled argon ion laser beam to the dye laser and to the delay line.

The 1 mm sample cell (Hellma, 110-QS) was not specifically selected due to the plano-parallelity of the optical window surfaces. Thus, there were only some positions on the windows allowing the laser to operate with maximum power.

The dye solution circuit was provided with a self-built damper to suppress the mechanical vibrations on the liquid column. The laser system achieved stable conditions after a warm-up time of about two hours.

The samples were ethanolic solutions ( $10^{-5}$  molar) of 1,4-dihydroxyanthraquinone. The sample material (Janssen Chimica, 96%) was used without any further purification. Only fresh prepared solutions were used to avoid adsorption effects inside the sample cell and the measuring flasks. The solutions were cautiously filled in since flow turbulences inside the cell caused long-lasting fluctuations of the intracavity light intensity.

Since intracavity spectroscopic methods stress molecules by intense irradiation, the resistance to photochemical decomposition of the molecules must be checked before experiments are started. This was carried out by irradiating the sample solutions with cw laser light (500 mW, 514.5 nm) for several hours. The stability of the compound was proved by periodic measurements of uv/vis-spectra.

UV/visible absorption spectra were recorded with the aid of Hewlett-Packard array spectrometer 8452A.

## 3 Results and Discussion

The frequencies of the argon ion laser emission coincide with the spectral region in which quinizarin absorbs. In this region, the room-temperature absorption spectrum of quinizarin dissolved in ethanol shows a weakly structured absorption band with maximum absorbance at 459.1 nm ( $20780 \text{ cm}^{-1}$ ). The first excited singlet state can be assigned as a  $\Pi-\Pi^*$  charge-transfer transition within the carboxyl group/hydroxyl group system [13, 14]. This property of the transition causes a nearly stable spectral position of the  $S_0-S_1$  absorption by changing solvents. For this reason, the spectrum obtained from an ethanolic solution is almost identical to a previously published spectrum of quinizarin dissolved in *n*-hexane [15]. The spectral location of the  $S_0-S_1$ , 0-0 transition was determined by inspecting the 2nd derivative of the absorption spectrum in order to identify weak transitions which exhibit shoulders on the inclining slope of the first strong absorption band and by consulting the fluorescence data. The fluorescence spectrum of the compound dissolved in *n*-hexane shows that the  $S_1-S_0$  0-0 transition is located at  $19131 \text{ cm}^{-1}$  [16]. Since energy gaps between absorption on-sets and on-sets in fluorescence do not exceed a few hundred wavenumbers and the 2nd derivative absorption spectrum reveals no additional transitions, the absorption band at  $19380 \text{ cm}^{-1}$  is assigned as 0-0 transition. Thus, using the 514.5 nm ( $19436 \text{ cm}^{-1}$ ) argon laser line for excitation, the excitation frequency closely corresponds to the on-set of the  $S_0-S_1$  transition.

Figure 3 shows results of the intracavity experiments. The amplification of the outcoupled dye laser power is expressed in terms of the intensity ratio  $(I - I_0)/I_0$  for each chosen wavelength.  $I_0$  is related to the laser emission of the sample-containing laser whose sample cell is not externally excited. The abscissa of the graphs covers the detectable spectral range ( $18657-17452 \text{ cm}^{-1}$ ) of the fluorescein dye laser output. Both graphs show limiting cases concerning possible time adjustment between the laser pulses: The curve de-

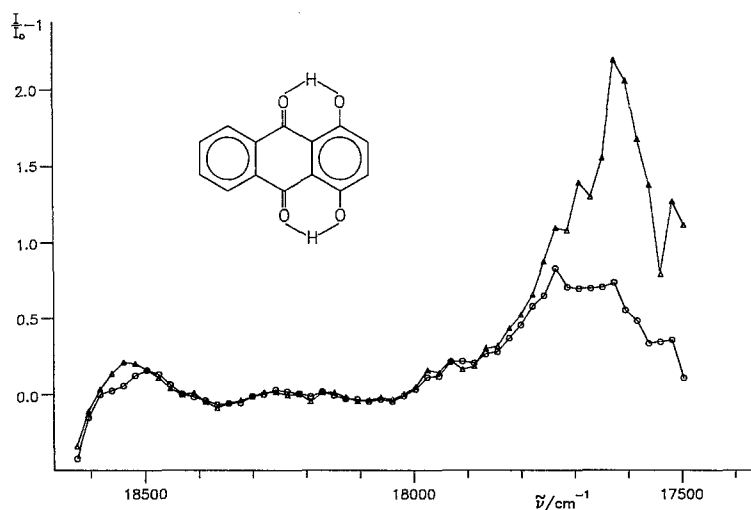


Fig. 3. The spectra of amplified laser output. The ordinate presents the increase of outcoupled dye laser power normalized to the intensity  $I_0$  of the laser without external excitation

pected by triangles is related to the case that the 10 ps pulse of the dye laser temporally overlaps with the 250 ps pulse of the  $\text{Ar}^+$  ion laser within the sample cell while the second curve represents the spectral laser output with absent temporal overlapping. In the latter case, the intracavity pulse is about 11 ns time-delayed in comparison to the excitation pulse of the argon ion laser. This delay is tuned to the repetition frequency of the optical pulses inside the dye laser resonator and results from the round-trip time minus the time between the first and the second pass through the sample cell.

In the case of simultaneous overlap of both pulses within the sample, maximum amplification of the laser output appears. At  $17614\text{ cm}^{-1}$ , the pulse intensity of the laser was more than threefold enhanced. The laser emission at wavenumbers greater than  $18657\text{ cm}^{-1}$  could not be amplified. In this region, the dye laser intensity even decreased as a result of exciting the sample by pulses of the argon ion laser. This effect appears in both spectra and can be interpreted as transient absorption. Absorptions generated by weak transitions (e.g., vibrational overtone transitions in solvent molecules) which are normally visible in intracavity absorption measurements equally affect  $I$  as well as  $I_0$  and do therefore not contribute to the shape of the laser amplification spectrum.

The spectrum of amplified dye laser output in the case of 11 ns time-delayed radiative deactivation is similarly shaped

to the room temperature spectrum of spontaneous fluorescence. This indicates that non-radiative relaxation processes in the solute/solvent system are already accomplished after 11 ns and the stimulated radiative deactivation of the excited quinizarin molecules by the time-delayed intracavity dye laser pulses starts from the non-vibrating equilibrium  $S_1$  state.

Non-radiative relaxation processes are apparently not accomplished in the case of imbedding the 10 ps probe pulse in the 250 ps pump pulse within the sample. Although, the resulting spectrum of amplified laser output is partially identical to the spectrum related to the delayed probe pulses, there are two spectral areas exhibiting significant alterations. Figure 4 shows the results of subtracting the spectrum related to the non-delayed probe pulses from the spectrum which belongs to the time-delayed probing. The transitions at  $18546\text{ cm}^{-1}$  and  $17614\text{ cm}^{-1}$  are attributed to induced fluorescence transitions which are generated from deactivating a certain vibronic state which is directly populated by argon ion laser emission. For this reason, the Stokes-shifts of both transitions ( $890\text{ cm}^{-1}$  and  $1822\text{ cm}^{-1}$ ) relative to the excitation wavenumber can be related to vibrational transitions in the ground-state molecule. Inspecting infrared and Raman spectra of the ground-state molecule, transitions at  $890\text{ cm}^{-1}$  and  $1822\text{ cm}^{-1}$  can not be identified as fundamen-

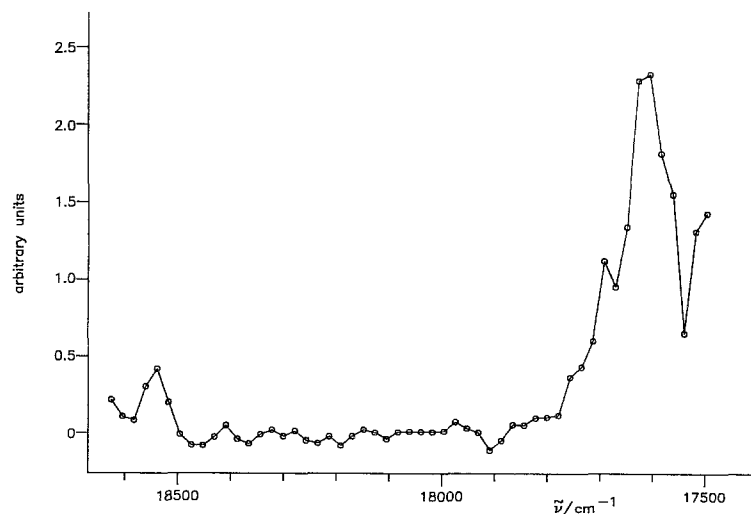


Fig. 4. Difference spectrum of amplified laser output. The spectrum obtained from temporal overlap of pump and probe pulses is subtracted from the spectrum related to maximum time-delayed probe pulses

tal modes or multiples of fundamental modes. Moreover, following the assignments of [15], there not any combination mode of non-totally symmetric vibrations does exist ( $a_2$ ,  $b_1$ , and  $b_2$  according to symmetry  $C_{2v}$  of quinizarin provided with two intramolecular hydrogen bonds) which yields totally symmetric vibrations of 890 or 1822  $\text{cm}^{-1}$ , respectively. Suitable numerical equivalence to the recorded data is only achieved by two pairs (459  $\text{cm}^{-1}$  + 430  $\text{cm}^{-1}$ ; 1398  $\text{cm}^{-1}$  + 430  $\text{cm}^{-1}$ ) of totally symmetric modes. The vibration at 1398  $\text{cm}^{-1}$  is characterized as a ring stretching vibration while the other two are in-plane angle deformation modes involving  $\delta$  (C=O) motions (459  $\text{cm}^{-1}$ ) and  $\delta$  (C–O) elongations (430  $\text{cm}^{-1}$ ) [15].

These combination modes also appear in the spectrum of spontaneous fluorescence but they exhibit negligible intensities [16].

In the  $S_1$  state, the energy of the in-plane C=O angle deformation mode increases to 488  $\text{cm}^{-1}$  while the energy of the C–O deformation mode remains stable [17]. Since the energetic difference between both deformation modes in  $S_1$  is accidentally equal to the difference between the excitation frequency and the frequency of the 0–0 transition it seems reasonable to assign the vibronic state from which the induced fluorescence starts as difference mode (488 – 430)  $\text{cm}^{-1}$ .

As an outlook, more detailed information about radiative transitions from vibronic states can surely be expected applying this method if two dye lasers are taken into account for the experimental setup. Then, the sample can be excited by shorter pulses of a second modelocked dye laser so that non-radiative competing processes, which become immediately active after excitation, are certainly reduced. Thus, there is a good chance to get a general idea of the

character of modes in excited states. This can be carried out by treating the enhanced laser output quantitatively in order to calculate transition moments with the use of multi-dimensional Franck-Condon analysis.

## References

1. S.L. Shapiro (ed.): *Ultrashort Light Pulses*, Topics in Applied Physics, Vol. 18 (Springer, Berlin, Heidelberg 1977)
2. G.R. Fleming: *Chemical Applications of Ultrafast Spectroscopy*, International Series of Monographs on Chemistry, Vol. 13 (Oxford, New York 1986)
3. T.D. Harris: Laser Intracavity-Enhanced Spectroscopy, in: *Ultra-sensitive Laser Spectroscopy*, ed. by D. Kliger (Academic, New York 1983)
4. H. Atampacher, H. Scheingraber, R.C. Vidal: *Phys. Rev. A* **32**, 254 (1985)
5. R.A. Keller, K.A. Truesdell: *J. Chem. Phys.* **75**, 4271 (1981)
6. W. Brunner, H. Paul: *Opt. Commun.* **12**, 252 (1974)
7. M. Maeda, F. Ishitsuka, Y. Miyazoe, M. Matsumoto: *Appl. Opt.* **16**, 403 (1977)
8. E. Kleist, H. Bettermann: *Opt. Letters* **13**, 449 (1988)
9. K.A. Truesdell, R.A. Keller: *Appl. Opt.* **22**, 339 (1983)
10. W.A. Renner: *The Chemistry of Antitumor Antibiotics*, Vol. 1 (Wiley, New York 1979)
11. H. Bettermann: Submitted to *J. Chem. Phys.*
12. G. Chini, K. Kelbert, H. Bettermann: *Rev. Sci. Instrum.* **62**, 1234 (1991)
13. Z. Yoshida, F. Takabayashi: *Tetrahydron* **24**, 933 (1968)
14. H. Inoue, T. Hoshi, T. Yoshino, Y. Tanizaki: *Bull. Chem. Soc. Japan* **45**, 1018 (1972)
15. G. Smulevich, L. Angeloni, S. Giovannardi, M.P. Marzocchi: *Chem. Phys.* **65**, 313 (1982)
16. T.P. Carter, G.D. Gillespie, M.A. Connolly: *J. Phys. Chem.* **82**, 192 (1982)
17. G. Smulevich, A. Amirav, U. Even, J. Jortner: *Chem. Phys.* **73**, 1 (1982)